Cellular Signalling 129 (2025) 111659

Contents lists available at ScienceDirect

Cellular Signalling

journal homepage: www.elsevier.com/locate/cellsig

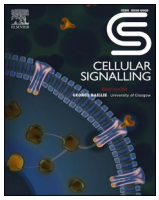

Enhancement of Ndrg2 promotes hypertrophic scar fibrosis by regulating PI3K/AKT signaling pathway

Boya Yu [a,b,*,1], Yalei Cao [c,1], Pianpian Lin [a,b], Lixia Zhang [a,b,*], Minliang Chen [a,b,*]

[a] Department of Plastic and Reconstructive Surgery, The Fourth Medical Center of Chinese PLA General Hospital, Beijing 100048, China
[b] Chinese PLA Medical School, Beijing 100853, China
[c] Department of Urology, Shandong Provincial Hospital Affiliated to Shandong First Medical University, Jinan, Shandong 250021, China

ARTICLE INFO

Keywords:
Hypertrophic scar
Skin fibrosis
Ndrg2
Fibroblast

ABSTRACT

Hypertrophic scar (HTS) is a prevalent chronic inflammatory skin disorder characterized by abnormal proliferation and extracellular matrix deposition. N-Myc downstream regulated gene 2 (Ndrg2) is a cell stress response gene related to cell proliferation, differentiation and various fibrotic diseases. However, the role of Ndrg2 in HTS is unknown and warrants further investigation. In this study, we confirmed that the expression of Ndrg2 was increased in HTS of human and a bleomycin-induced fibrosis mouse model. We then used Ndrg2 knockout mice and found Ndrg2 deletion could significantly reduce the synthesis of collagen and alleviate skin fibrosis. In addition, the proliferation and migration of Ndrg2-interfered HTS-derived fibroblasts decreased and those of Ndrg2-overexpressed normal skin-derived fibroblasts increased. Further, by western blot analysis, we verified that the expression of phosphorylated-PI3K, PI3K, phosphorylated-AKT and AKT were all increased after Ndrg2 overexpressed in normal skin-derived fibroblasts. Moreover, PI3K inhibitor (LY294002) administration significantly rescued the effect of Ndrg2 overexpression on skin fibrosis. In summary, our results demonstrated that Ndrg2 could promote HTS fibrosis by mediating PI3K/AKT signaling pathway. Our data suggest that Ndrg2 may be a promising therapeutic target for HTS.

1. Introduction

Hypertrophic scar (HTS) is a pathological result of excessive wound healing after skin injury, mainly composed of structural abnormalities and excessive generation of collagen fibers [1], often secondary to burns, trauma, and surgery [2]. The clinical manifestation of HTS is tissue thickening with hardened texture, often accompanied by symptoms including pruritus and pain [3]. In severe cases, it not only affects the patient's quality of life but also brings a heavy psychological burden to the patient. There are many treatments for hypertrophic scars [4,5], including compression therapy, drug injection, radiation therapy, laser therapy, and surgical resection, but their efficacy is limited and the recurrence rate is high [6]. Therefore, in-depth research on the pathogenesis of hypertrophic scars is significant for the treatment.

Fibroblasts are considered the predominant effector cells involved in the development of hypertrophic scars, capable of producing and reshaping the extracellular matrix [7]. Changes in their biological behaviors including proliferation, migration, apoptosis, and transformation have significant effects on scar formation [8]. Hence, many scholars have focused their research on fibroblasts and explored the role of their involved signaling pathways in scar formation, such as the TGF-β/Smad and PI3K/AKT pathways [9–14].

N-Myc downstream regulated gene 2 (Ndrg2) is a member of the Ndrg gene family and can be transcribed into a mRNA of 2024 bp [15]. The gene encodes a 40.7 kD protein of 371 amino acids with an α/β hydrolase catalytic domain [16]. Previous studies have shown that the *Ndrg2* gene is a cell stress response gene that is associated with cell proliferation, differentiation, and apoptosis and plays an antitumor role

Abbreviations: BLM, bleomycin; CCK-8, Cell Counting Kit-8; DMSO, Dimethyl sulfoxide; EdU, 5-ethynyl-2′-deoxyuridine; H&E, hematoxylin–eosin; HFB, HTS-derived fibroblast; HTS, hypertrophic scar; IHC, immunohistochemistry; MMP2, matrix metallopeptidase 2; Ndrg2, N-Myc downstream-regulated gene 2; NFB, normal skin-derived fibroblast; NS, normal skin; PMSF, phenylmethanesulfonyl fluoride; TIMPs, metalloproteinases; WT, wild type..

* Corresponding authors at: Department of Plastic and Reconstructive Surgery, The Fourth Medical Center of Chinese PLA General Hospital, Beijing 100048, China.
E-mail addresses: yby0507@163.com (B. Yu), vivian-0506@163.com (L. Zhang), chenml@sohu.com (M. Chen).

[1] These authors contribute equally to this work.

https://doi.org/10.1016/j.cellsig.2025.111659
Received 15 November 2024; Received in revised form 17 January 2025; Accepted 12 February 2025
Available online 14 February 2025

in various cancer types [17–19]. Studies have indicated that Ndrg2, as a tumor suppressor, can inhibit the epithelial mesenchymal transition in breast cancer [20] and gallbladder cancer [21]. Ndrg2 is also associated with organ damage repair and various fibrotic diseases and can also inhibit TGF-β1/Smad pathway to alleviate liver fibrosis [22]. However, upregulation of Ndrg2 expression can cause fibrosis of human lens epithelial cells [23]. There are no reports on the research of Ndrg2 in skin tissue fibrosis.

In this study, we investigated the protein expression of Ndrg2 in HTS of human and bleomycin-induced fibrosis mouse models. We further explored the effect of Ndrg2 on the biological function of fibroblasts. By knocking down Ndrg2 in HTS-derived fibroblast (HFB) and over-expressing Ndrg2 in normal skin-derived fibroblast (NFB), we validated our hypothesis that Ndrg2 can promote the proliferation and migration of fibroblasts through the PI3K/AKT signaling pathway. Our results underscore Ndrg2 as a novel target gene in HTS, offering new insights into signaling mechanisms and potential targets for the clinical management of HTS.

2. Materials and methods

2.1. Collection of tissues sample from human

HTS and normal skin tissues were collected from patients during plastic surgery. The samples were divided into three parts for histochemical stain, protein extraction and isolating fibroblasts. Then the samples were stored in −80 °C until use. This study was approved by the Medical and Ethics Committees of the Fourth Medical Center of Chinese PLA General Hospital (2023KY140-KS001), and written informed consent was obtained from each patient before enrolling in this study.

2.2. Animal model

8-week-old male adult C57BL/6 wild type (WT) mice and Ndrg2 knockout ($Ndrg2^{-/-}$) mice were included in this study. C57BL/6 mice were purchased from Ke Yu Laboratory Animal Center of Beijing and $Ndrg2^{-/-}$ mice were purchased from Shanghai Model Organisms Center. According to the manufacturer's protocol, Quick Genotyping assay kit for mouse tails (D7283, Beyotime, Shanghai, China) was used to identify PCR-based genotyping (Fig. S1). Specific primers were synthesized by Sangon Biotech (Shanghai, China) and the primer sequences are listed in Table S1. All mice were raised facility of the Fourth Medical Center, Chinese PLA General Hospital for one week before the experiment. C57BL/6 mice and $Ndrg2^{-/-}$ mice were randomly divided into two groups, one group was injected with bleomycin (BLM), and the other was injected with PBS (WT + PBS, WT+ BLM, $Ndrg2^{-/-}$ + PBS and $Ndrg2^{-/-}$ + BLM). The mice in the BLM group were subcutaneously injected with 100 μl BLM (100 μg/ml) daily, while mice in the control group received equal volumes of PBS. After four weeks, all mice were euthanized and skin tissues were obtained for following experiments. The animal experiments were approved by the Experimental Animal of Committee Fourth Medical Center, Chinese PLA General Hospital (SQ2023662).

2.3. Hematoxylin-eosin and Masson staining

The collected samples from human and mice were fixed in 4 % paraformaldehyde solution and dehydrated with ethanol series. Then the fixed tissues were embedded in paraffin and sectioned into 5-μm-thick paraffin sections, which were stained with the hematoxylin and eosin staining kit (AR1180, Boster Biological Technology, Wuhan, China) and Masson staining kit (G1340; Solarbio, Beijing, China), respectively, according to the manufacturer's instructions. We scaned the images with digital panoramic scanner (WS-10, WISLEAP, Zhiyue Medical Technology Co., LTD; Jiangsu, China). Relative collagen content was quantified by comparing optical density values using Image J.

2.4. Western blot analysis

The proteins were extracted from HTS, normal skin tissues, skin of experimental mice (tissues) or cells in ice-cold RIPA lysis buffer (P0013B, Beyotime, Shanghai, China) containing 1 mM phenylmethanesulfonyl fluoride (PMSF). Protein levels were measured with a bicinchoninic acid (BCA) assay kit (Pierce/Thermo Scientific). Protein samples were denatured and then separated through 10 % SDS-PAGE gels and transferred onto a PVDF membrane (Bio-Rad, Hercules, CA). Blocked the membranes with 5 % defatted milk in TBST buffer (B1009, Applygen, Applygen Technologies Inc. Beijing, China) for 1 h at room temperature and then incubated with the following primary antibodies at 4 °C overnight: rabbit polyclonal to Ndrg2 (1:1000, 5667, Cell Signaling Technology, Danvers, MA, USA); rabbit polyclonal to COL1A1 (1:1000, 72,026, Cell Signaling Technology, Danvers, MA, USA); rabbit polyclonal to p-PI3K (1:1000, 4228, Cell Signaling Technology, Danvers, MA, USA); rabbit polyclonal to PI3K (1:1000, 4249, Cell Signaling Technology, Danvers, MA, USA); rabbit polyclonal to p-AKT (1:1000, 4060S, Cell Signaling Technology, Danvers, MA, USA); rabbit polyclonal to AKT (1:1000, 9272S, Cell Signaling Technology, Danvers, MA, USA); and mouse monoclonal to GAPDH (1:3000, HC301–01, TransGen Biotech, China), respectively. After washing with TBST, the blots were incubated in horseradish peroxidase-conjugated secondary antibody including goat anti-rabbit IgG antibody (1:5000, BF03008, Biodragon Immunotechnologies, Suzhou, Jiangsu, China) or goat anti-mouse IgG antibody (1:5000, BF03001, Biodragon Immunotechnologies) for 2 h at room temperature. Protein bands were scanned with an enhanced chemiluminescence detection kit (Pierce) followed by using a Tanon 5200 chemiluminescence detection system (Tanon, Shanghai, China). Protein levels were quantified by comparing the grey value with a computer-assisted imaging analysis system (Image J, NIH).

2.5. Immunohistochemistry staining

Paraffin sections were prepared as described previously. The sections were dewaxed, rehydrated, antigen repaired and incubated by anti-Ndrg2 antibody (1:200, 5667, Cell Signaling Technology, Danvers, MA, USA) and secondary antibody. DAB reagent was used to colored and hematoxylin was applied to counterstained. Finally, the slides were observed with digital panoramic scanner (WS-10, WISLEAP, Zhiyue Medical Technology Co., LTD; Jiangsu, China).

2.6. Cell isolation, culture and identification

The dermal tissues of HTS or normal skin were rinsed with sterile PBS containing penicillin–streptomycin and minced into small pieces (~ 1 mm). Then the pieces were incubated in Dulbecco's Modified Eagle Medium (DMEM, Gibco, Grand Island, New York, USA) containing 10 % fetal bovine serum and 1 % penicillin–streptomycin at 37 °C in an atmosphere of 5 % CO_2. The medium was replaced every 2–3 days. Explanted tissues were removed when cells proliferated from the edge of tissue (approximately 7–10 days). When the density of cells reached more than 80 %, the cells were subcultured. Cells from the third to the fifth passages were used for experiments. Fibroblasts cultured in fluorescent dishes were fixed in paraformaldehyde for 15 min. After rinsing with PBS, 0.5 % Triton X-100 was used to permeabilize for 15 min at room temperature. Then the fibroblasts were incubated for 1 h with 3 % goat serum to block nonspecific binding sites at room temperature. Cells were again washed with PBS and incubated with the specific primary antibody against vimentin (1:1000, 5741, Cell Signaling Technology, Danvers, MA, USA) at 4 °C overnight. Primary antibodies were detected with Alexa Fluor 488 conjugated secondary antibodies (1:200, ab150117; Abcam). DAPI (Thermo Fisher, Waltham, MA, USA) was used to visualize nuclear. Finally, images were obtained with a confocal microscope (Zeiss LSM880, Carl Zeiss Microscopy GmbH, Jena, Germany). Fibroblasts with green cytoplasm were regarded as positive cells, and 10

fields were randomly selected to record the number of positive cells for evaluating (Fig. S2).

2.7. Cell treatment

The Ndrg2 knockdown and Ndrg2 overexpressing adenoviruses were constructed by Hanbio Biotechnology Co., Ltd. (Shanghai, China). According to the manufacturer's recommendations, cells were cultured in 60 mm-dishes and the appropriate adenoviruses (multiplicity of infection = 25) were added into the dishes when confluence reaching 60 %–70 %. 24 h later, the medium containing adenovirus was discarded and replaced with fresh medium. When the cells overgrew the bottom of the dish, puromycin (Solarbio, Beijing, China) was used to select stably infected cells. The efficiency of knockdown and overexpression were evaluated by Western Blot. Finally, hypertrophic scar-derived fibroblasts with down-regulation of Ndgr2 and normal skin-derived fibroblasts with overexpression of Ndrg2 were obtained for further experiments. Western blot was used to assessed the protein levels of phosphorylated and total PI3K or AKT in HFB with down-regulation of Ndgr2 and NFB with overexpression of Ndrg2. To investigate whether the effect of Ndrg2 on proliferation and migration is mediated through PI3K/AKT pathway in fibroblast, we treated NFB with overexpression of Ndrg2 with a PI3K inhibitor, LY294002 (HY-10108, MCE, USA), and assessed the ability of cell proliferation and migration.

2.8. Cell counting Kit-8 assay

According to the manufacturer's protocol, the cells in different groups were seeded in 96-well plates at a density of 4×10^3 cells /ml and cultured at 37 °C for 24-, 48-, and 72-h, respectively. After that, 10 μl Cell Counting Kit-8 (CCK-8) solution (CK04, Dojindo Laboratories, Japan) and 90 μl complete medium were added to each well. The absorbance at 450 nm was measured with a microplate reader and analyzed after incubation at 37 °C for 2 h.

2.9. Transwell assay

Transwell assay was conducted using a transwell chamber with a membrane pore size of 8 μm (membrane diameter 6.5 mm, Corning Corporation, USA). Cell suspensions (1×10^4 cells) diluted in serum-free DMEM were seeded in the upper chamber. Lower chamber was added with DMEM containing 20 % FBS. The cells in the upper chamber were removed after 24 h, and the migrated cells were fixed with 4 % paraformaldehyde for 30 min, stained with 0.1 % crystal violet for 20 min. After washing with PBS, the number of migrating cells was calculated through an optical microscope.

2.10. Wound-healing assay

5×10^5 cells per well were seeded in 6-well plates, and linear defects were generated on the cell surface using sterile 200-μl pipettor tip when cells reached approximately 100 % confluence. Floating cells were gently washed away using sterile PBS. Then the cells were subsequently cultured with a serum-free medium. The scratch distance pictures were taken by light microscope at 0- and 48-h time points, and measured with Image J software.

2.11. Transcriptome profiling

RNA-seq analysis was performed in HFB infected with the control shRNA adenovirus vector and Ndrg2 shRNA groups. Total RNA was extracted using Trizol reagent (Thermo Fisher, 15,596,018) following the manufacturer's procedure. Then, mRNA was purified from total RNA (5 μg) by using Dynabeads Oligo (dT) (Thermo Fisher, CA, USA) with two rounds purification. The cDNA samples were sequenced using the Agilent Bioanalyzer 2100 system (Agilent Technologies, CA, USA). We performed the 2 × 150 bp paired-end sequencing (PE150) on an Illumina Novaseq™ 6000 (Novogene Co, Ltd., Beijing, China) following the vendor's recommended protocol.

2.12. Statistical analysis

Statistical analyses were performed with GraphPad Prism 9.0 for Windows (GraphPad Software, La Jolla, CA). All quantitative biochemical data and immunofluorescence staining were representative of at least three independent experiments. Two-tailed unpaired Student's *t*-test was used for the comparison of the mean values between two groups. All results were presented as the means ± SEM, and differences with $p < 0.05$ were considered statistically significant. The significant differences between groups were represented as * $p < 0.05$, ** $p < 0.01$ and *** $p < 0.001$.

3. Results

3.1. Expression of Ndrg2 was upregulated in HTS of patients

We collected HTS tissues and normal skin (NS) tissues from patients. The excess adipose layer was shaved, then epidermal and dermis layer was left and used to perform hematoxylin-eosin (H&E) and Masson staining. H&E staining revealed that the dermal thickness of HTS tissues was thicker than that of NS tissues (Fig. 1A and B). In addition, Masson staining identified disorderly collagen fibers and highlighted significant collagen production in the HTS group compared with the NS group (Fig. 1A and C). The protein expression levels of Ndrg2 and collagen I in HTS compared with the matched NS were detected using western blot. The results indicated the protein expression levels of Ndrg2 and collagen I were significantly upregulated in the HTS group compared with the NS group (Fig. 1D-F). In particular, immunohistochemistry (IHC) of Ndrg2 revealed stronger expression in the dermis of HTS than that in the NS group (Fig. 1G and H). These results indicated that Ndrg2 expression was increased in the skin of HTS, suggesting the important role of Ndrg2 in skin fibrosis.

3.2. Increased expression of Ndrg2 in the BLM induced fibrosis mouse model

To further clarify the role of Ndrg2 in skin fibrosis, a fibrosis model was constructed by persistent bleomycin injection into the dermis of C57BL/6 mice as previous studies have described [24]. At 28 days after modeling, dermal tissues were collected for subsequent testing (Fig. 2A). A histological analysis was conducted to explore the effect of bleomycin (BLM) on skin fibrosis. H&E and Masson's staining revealed that BLM-treated mice exhibited increased dermal thickness and collagen content compared with the PBS-treated group (Fig. 2B-D). To detect the expression of Ndrg2 in the skin of BLM-treated mice, IHC staining and western blot were conducted. The IHC staining revealed higher level of Ndrg2 expression in the dermis of BLM-treated mice than in PBS-treated mice (Fig. 2B and E). Consistently, high levels of Ndrg2 and collagen I protein were detected in BLM-treated mice compared with the PBS-treated group (Fig. 2F-H). Collectively, these results demonstrated that the protein expression of Ndrg2 was elevated and collagen increased in a BLM-induced fibrosis mouse model, which suggested that Ndrg2 may promote the development of skin fibrosis.

3.3. Loss of Ndrg2 alleviated skin fibrosis in the BLM-induced mouse model

To demonstrate the effect of Ndrg2 on skin fibrosis, we compared the BLM-induced skin fibrosis in Ndrg2 knockout mice (KO + BLM) and wild-type mice (WT + BLM). We continually injected BLM into the dermis of WT and Ndrg2 KO mice for 28 days, and then we collected their skin tissues (Fig. 3A). As revealed by H&E and Masson staining,

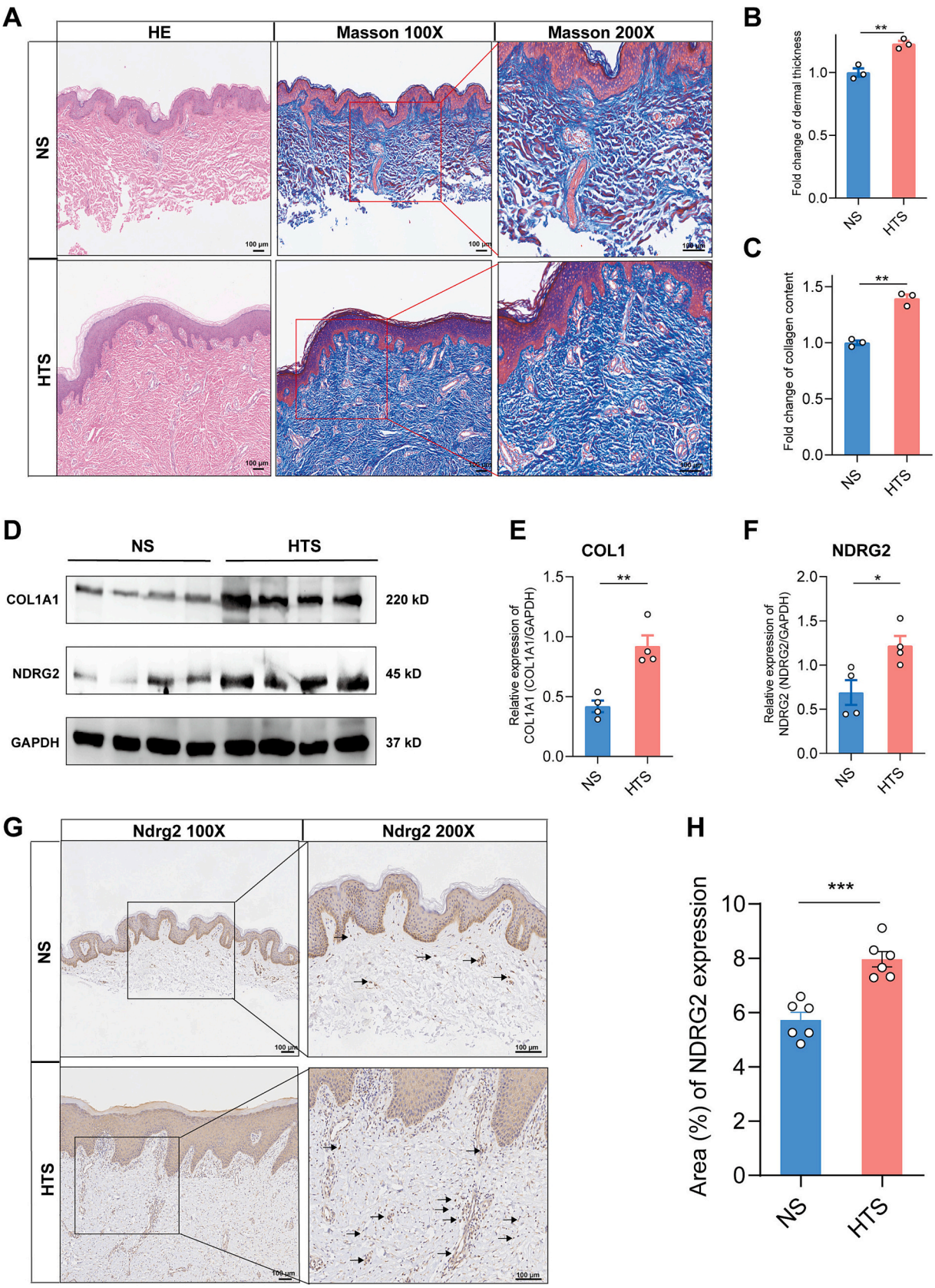

Fig. 1. Changes in histological features and enhanced Ndrg2 expression in HTS. (A) H&E and Masson staining of skin tissues in NS and HTS. Scale bar = 100 μm, as indicated. (B-C) Fold change of dermal thickness (B) and collagen content (C) of NS and HTS tissues determined from photomicrographs using ImageJ. (D-F) Representative images and data analysis of protein expression of COL1A1 and NDRG2 in skin tissues of NS and HTS; $n = 4$ per group. (G) IHC staining for Ndrg2 in the NS and HTS groups; the black arrow indicates Ndrg2-positive cells. Scale bar = 100 μm, as indicated. (H) Area (%) of NDRG2 expression in NS and HTS groups. All data are presented as mean ± SEM. $^{*}p < 0.05$; $^{**}p < 0.01$. All data were analyzed using a two-tailed unpaired Student's *t*-test.

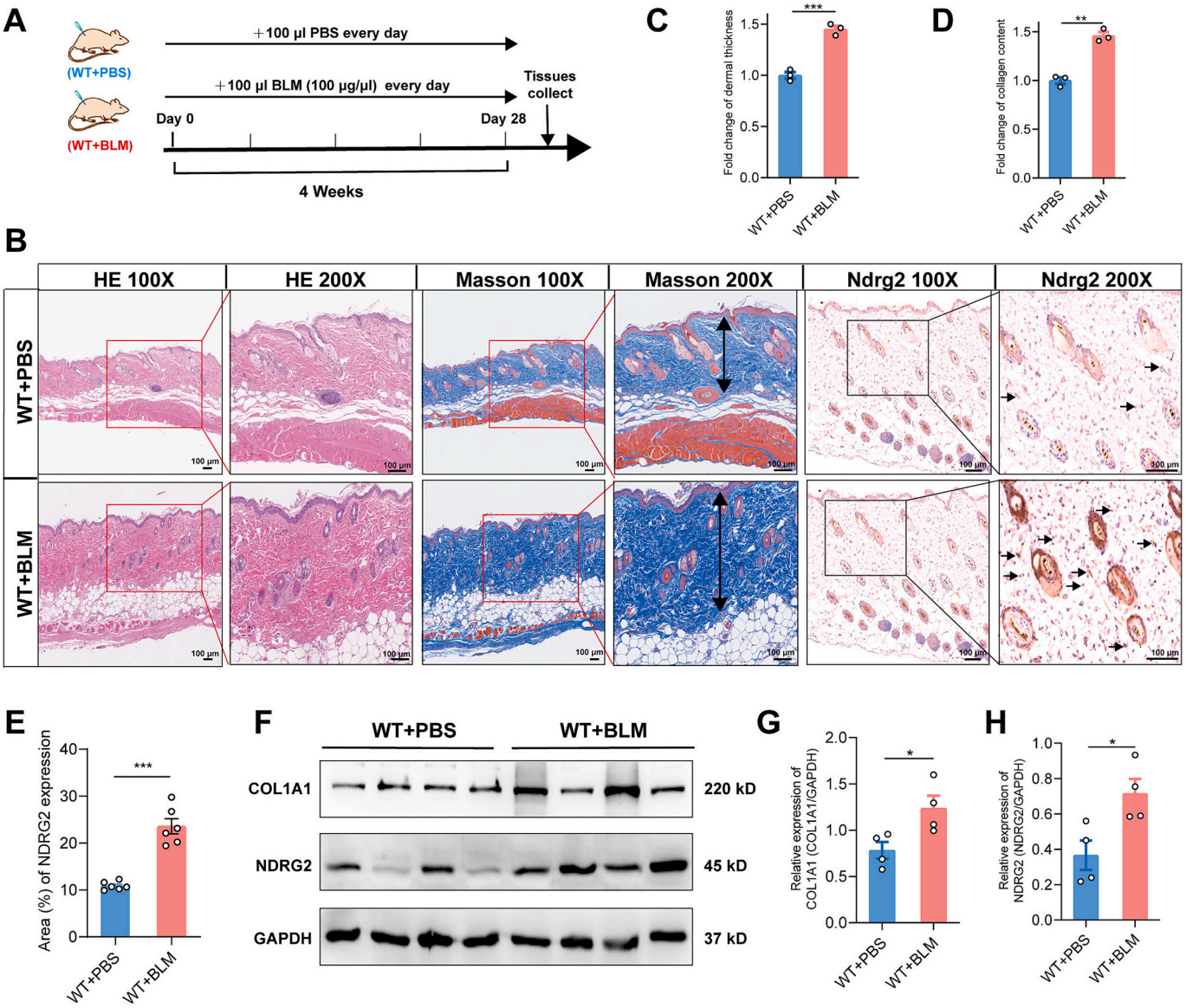

Fig. 2. Enhanced Ndrg2 in the BLM-induced fibrosis mouse model. (A) The schematic illustration of the experimental mouse model. (B) Sections were stained with H&E and Masson's trichrome, and IHC staining of the WT + PBS and WT + BLM groups was conducted. The black arrow indicates Ndrg2-positive cells. (C-D) Fold change in dermal thickness (C) and collagen content (D) in the WT + PBS and WT + BLM groups was calculated. (E) Area (%) of NDRG2 of the WT + PBS and WT + BLM groups. (F-H) Representative images and data analysis of protein expression of COL1A1 and NDRG2 in mouse skin measured by western blot; $n = 4$ per group. All data were analyzed as mean ± SEM. $^{*}p < 0.05$; $^{**}p < 0.01$; ***, $p < 0.001$. All data were analyzed using a two-tailed unpaired Student's *t*-test.

Ndrg2 knockout in BLM-induced fibrotic skin resulted in a thinner epidermis and dermis, less collagen deposition, and a more ordered arrangement of collagen structures (Fig. 3B-D). The IHC staining revealed no Ndrg2-positive cells in the dermis of KO mice because Ndrg2 was knocked out. However, the level of Ndrg2 expression was high in the dermis of WT mice (Fig. 3B and E). We further investigated the protein expression of collagen I and Ndrg2 in the two groups. As expected, the protein levels of COL1A1 and Ndrg2 in the lesion skin of KO + BLM both significantly decreased compared with those of BLM-treated WT mice (Fig. 3F-H). Taken together, Ndrg2 knockout may improve the collagen structure arrangement and proportion and decrease myofibroblasts in a BLM-induced fibrosis mouse model.

3.4. *Knockdown Ndrg2 inhibited the proliferation and migration of HTS-derived fibroblasts*

To verify the regulatory effect of Ndrg2 on fibrosis, we constructed Ndrg2 shRNA to exogenously alter the expression of Ndrg2 in primary human fibroblasts, which were cultured from HTS. We infected HFB with the control shRNA adenovirus vector (shNC group) and Ndrg2 shRNA (shNdrg2 group) specifically. Based on the western blot, Ndrg2 expression was significantly downregulated in HFB (Fig. S3). First, we observed that the cell viability of the shNdrg2 group was significantly reduced compared with that of the shNC group (Fig. 4A). To further illustrate the growth effect of Ndrg2, we performed EdU staining to detect the proliferation ability of fibroblasts treated with shNC or shNdrg2. The relative ratio of EdU-positive cells in the shNdrg2 group was remarkably decreased compared with that in the shNC group (Fig. 4B and C). The results of the Transwell and wound-healing assay indicated that the capacities of both invasion and migration were considerably reduced in the shNdrg2 group compared with the shNC group. All of these experimental findings demonstrated that knockdown of Ndrg2 inhibited the proliferation and migration of HFB.

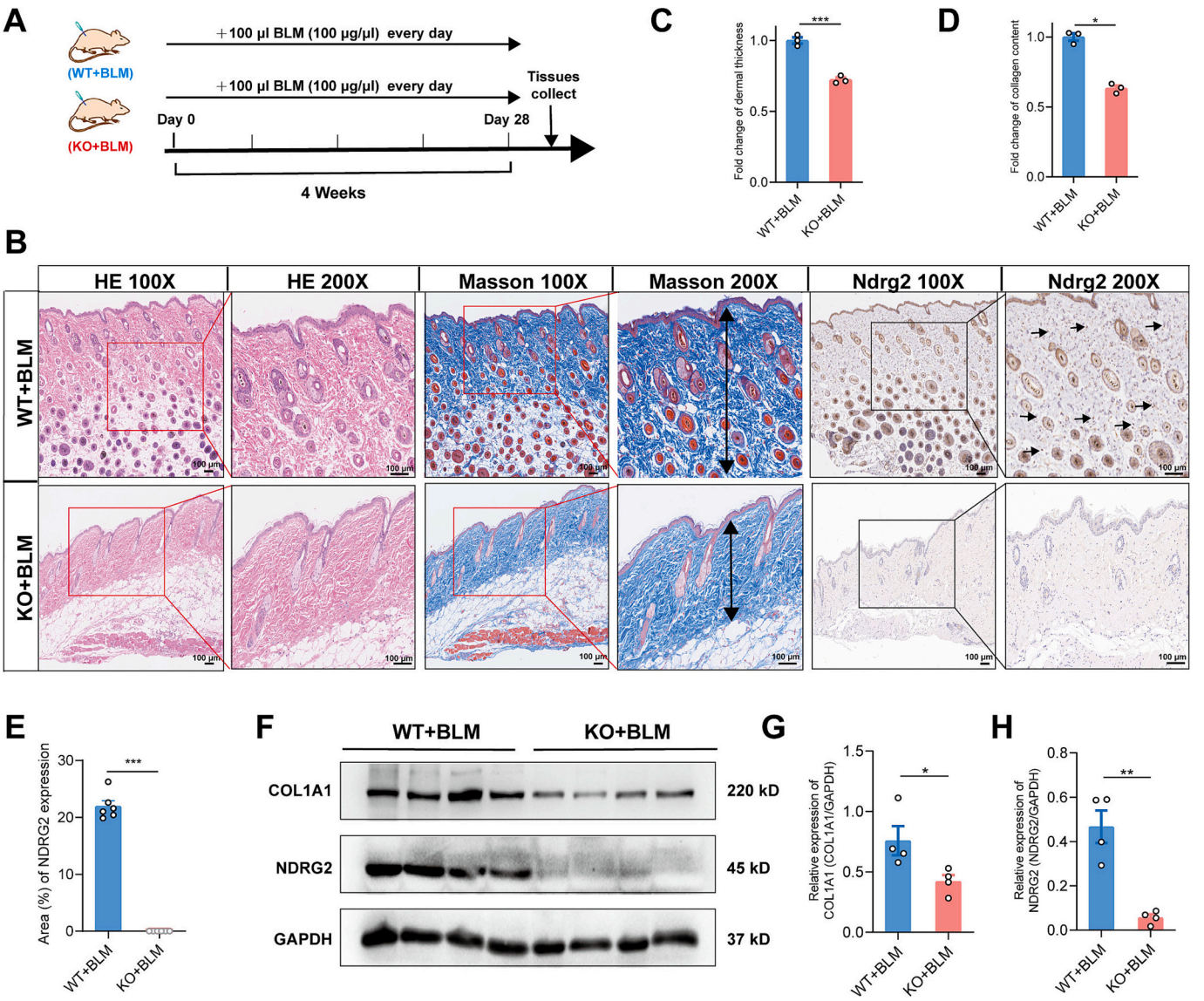

Fig. 3. Knockout Ndrg2 alleviated skin fibrosis in the BLM-induced fibrosis mouse model. (A) The protocol of the experimental mouse model. Bleomycin was continually injected into WT and Ndrg2 knockout mice for 4 weeks. (B) Sections were stained with H&E and Masson's trichrome, and IHC staining of WT + BLM and KO + BLM groups was conducted. The black arrow indicates Ndrg2-positive cells. (C-D) Fold change in dermal thickness (C) and collagen content (D) in the WT + BLM and KO + BLM groups were calculated. (E) Area (%) of NDRG2 expression in the WT + BLM and KO + BLM groups. (F) Representative images and data analysis of protein expression of COL1A1 and NDRG2 in mouse skin measured by western blot; $n = 4$ per group. All data are presented as mean ± SEM. $^{*}p < 0.05$; $^{**}p < 0.01$; ***, $p < 0.001$. All data were analyzed using a two-tailed unpaired Student's *t*-test.

3.5. *Overexpression of Ndrg2 enhanced the proliferation and migration of normal skin-derived fibroblasts*

Next, Ndrg2-overexpressing adenovirus with enhanced green fluorescent protein was transfected into NFB (Fig. S4A). Transfection efficiency was confirmed by western blot. As expected, the protein expression level of Ndrg2 was significantly upregulated in the overexpressing group (Over) compared with the negative vector group (Vector) (Fig. S4B). Our Cell Counting Kit-8 (CCK-8) assays revealed that Ndrg2 overexpression promoted the proliferation of NFB (Fig. 5A). Then, EdU staining was conducted and revealed Ndrg2 overexpression significantly promoted the proliferation of NFB (Fig. 5B and C). Wound-healing assay and Transwell assay were used to determine the migration and invasion potential of cells in the Vector and Over groups, respectively. It was found that following Ndrg2 overexpression, the capacity of NFB to invade was considerably elevated (Fig. 5D and E). Meanwhile, Ndrg2 overexpression promoted the migration ability of NFB (Fig. 5F and G). Together, these results indicated that Ndrg2 was capable of promoting proliferation and migration of NFB and contributed to skin fibrosis.

3.6. *Ndrg2 regulated the PI3K/AKT signaling pathway in fibroblasts*

Given that the PI3K/AKT signaling pathways is closely associated with HTS as our previous research reported [25], we assumed that the prevention of fibrosis by Ndrg2 interference may act through the PI3K/AKT pathway. To confirm this hypothesis, we conducted RNA-seq in HFB from shNC and shNdrg2 groups. PCA showed that shNC and shNdrg2 had clear differences in clustering characteristics (Fig. 6A). A total of 1692 DEGs were identified in shNdrg2 group compared to shNC, including 883 downregulated and 809 upregulated genes (Fig. 6B). Additionally, the heatmap showed that PI3K/AKT pathway-related genes such as *Pten*, *Pdk1* and *Tlr4* was altered in shNdrg2 group (Fig. 6C). Furthermore, western blot was performed in HFB and NFB

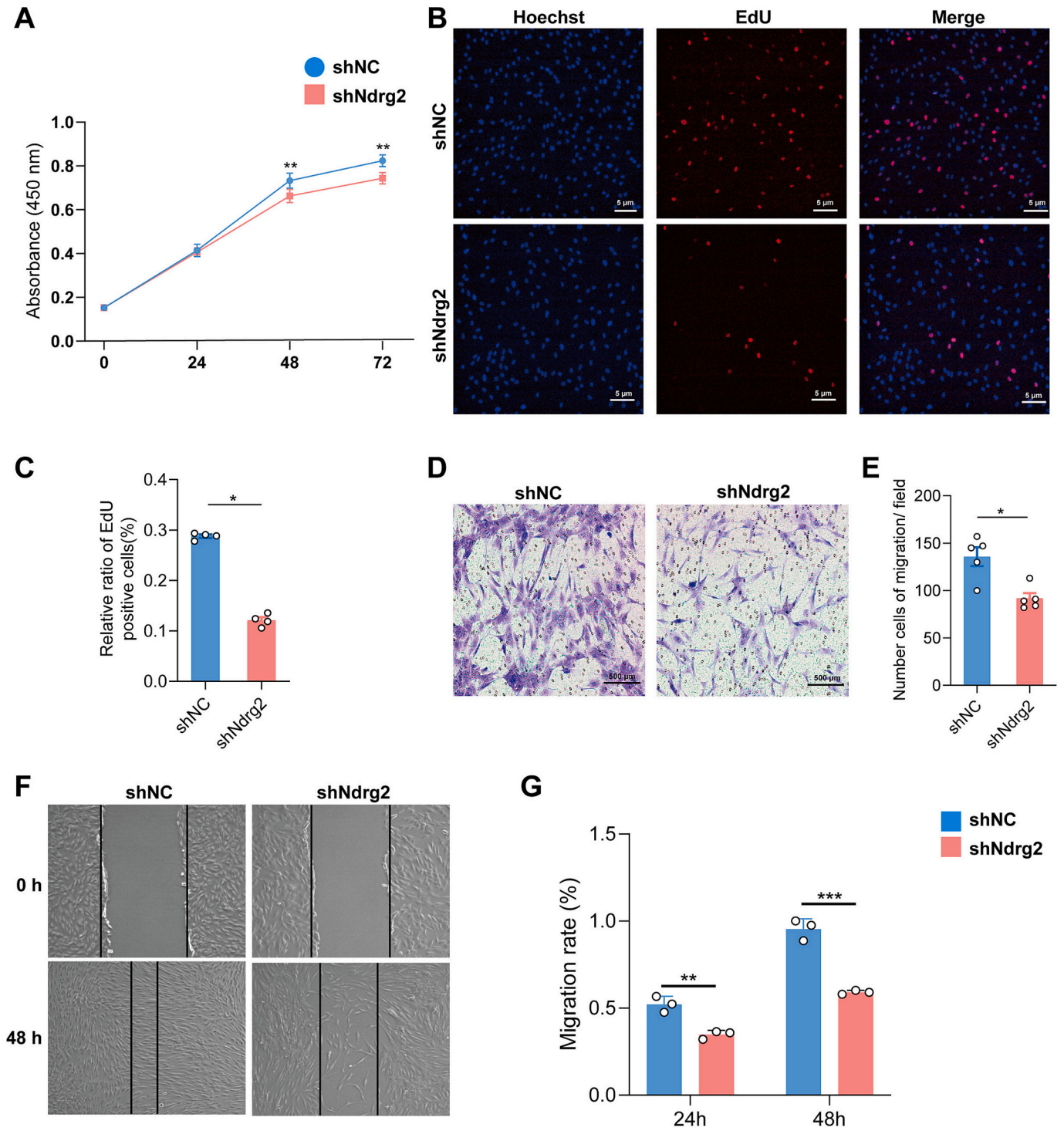

Fig. 4. Knockdown Ndrg2 inhibited the proliferation and migration of fibroblasts. (A) The cell viability of fibroblasts treated with shNC or shNdrg2; $n = 6$ per group. (B) EdU staining was performed to detect the proliferation ability of fibroblasts treated with shNC or shNdrg2. Scale bar = 5 μm. (C) The relative ratio of EdU-positive cells in the shNC and shNdrg2 groups; $n = 4$ fields per group. (D-E) Quantification analysis of number cell of migration per field (D) and representative images of Transwell invasion assay (E) in the two groups; $n = 5$ fields per group. (F-G) Wound-healing assay was performed to detect the effect of cell migration in the shNC and shNdrg2 groups. All data are presented as mean ± SEM. $^{*}p < 0.05$; $^{**}p < 0.01$; ***, $p < 0.001$. All data were analyzed using a two-tailed unpaired Student's *t*-test.

with Ndrg2 interference and overexpression, respectively. The results verified that Ndrg2 interference in HFB exhibited lower levels of Ndrg2 expression and protein phosphorylation in the PI3K/AKT pathway compared with the shNdrg2 group (Fig. 6D-G). By contrast, after overexpression of Ndrg2 in NFB, the protein level of Ndrg2 was significantly upregulated. In addition, overexpressing Ndrg2 dramatically increased the phosphorylation levels of PI3K and AKT (Fig. 6H-K). Collectively, our findings suggested that Ndrg2 may regulate the PI3K/AKT pathway in fibroblasts.

3.7. PI3K inhibitor (LY294002) decreased proliferation and invasion of Ndrg2 overexpressed NFB

To further explore whether Ndrg2 regulates fibroblasts through the

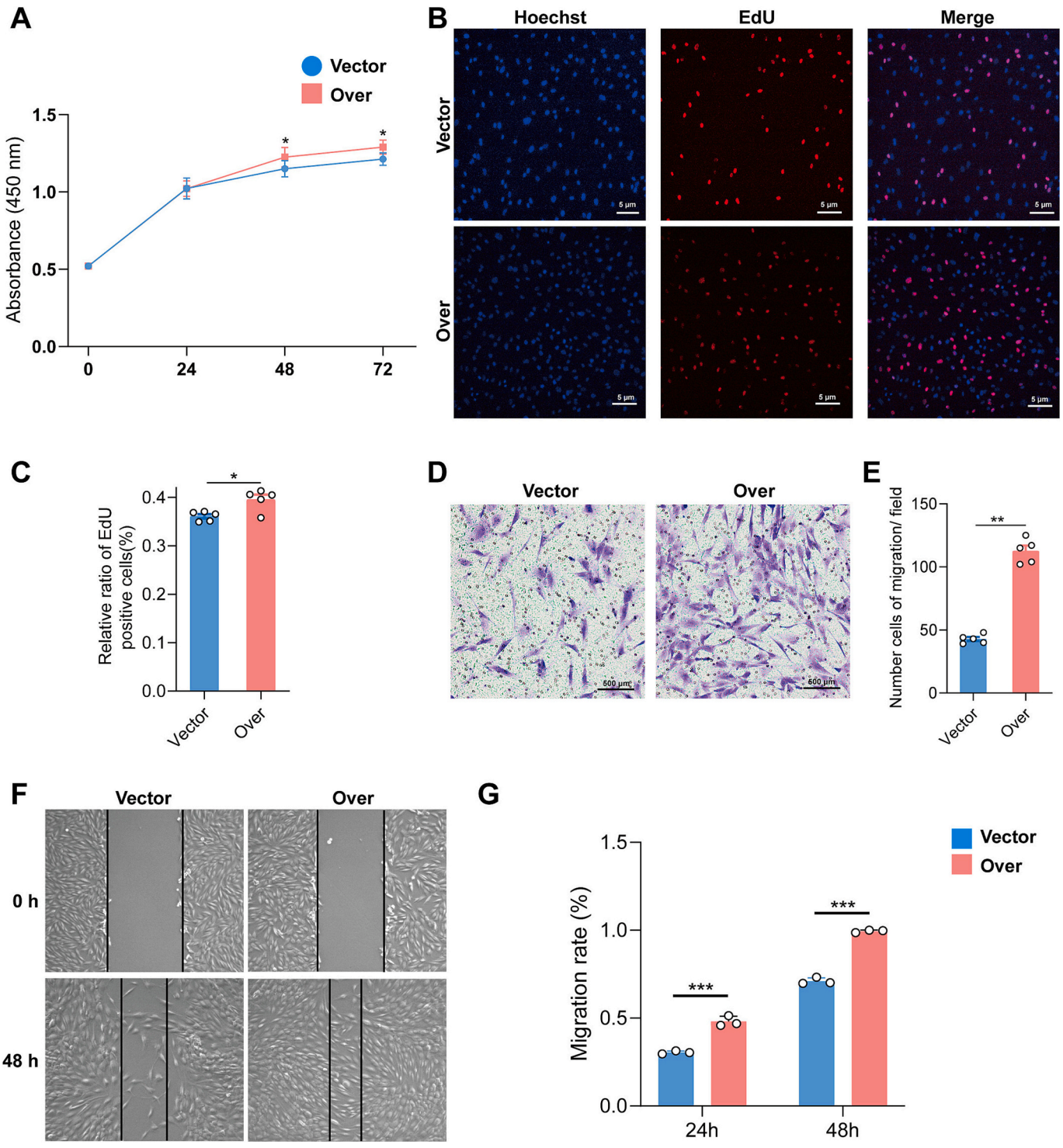

Fig. 5. Overexpression of Ndrg2 promoted the proliferation and migration of fibroblasts. (A) The cell viability of fibroblasts treated with Vector or Ndrg2-overexpressing adenovirus (Over); $n = 5$ per group. (B) Representative images of EdU staining of fibroblasts treated with Vector or Ndrg2-overexpressing adenovirus. Scale bar = 5 μm. (C) The relative ratio of EdU-positive cells in the Vector and Over groups; n = 5 fields per group. (D-E) Quantification analysis of cell migration per field (D) and representative images of Transwell invasion assay (E) in the Vector and Over groups; n = 5 fields per group. (F-G) Wound-healing assay was performed to detect the effect cell migration in Vector and Over groups. All data are presented as mean ± SEM. *$p < 0.05$; **$p < 0.01$; ***, $p < 0.001$. All data were analyzed using a two-tailed unpaired Student's *t*-test.

PI3K/AKT pathway, we overexpressed Ndrg2 and then used an inhibitor (LY294002) of PI3K to verify its effects on the proliferation and invasion of NFB. First, the results of western blot indicated that the ratios of p-PI3K/PI3K and p-AKT/AKT were significantly downregulated after using LY294002 in Ndrg2-overexpressed NFB (Fig. 7A-C). The results of CCK-8 experiments indicated that the cell viability was relatively decreased after the treatment of LY294002 in Ndrg2-overexpressed NFB (Fig. 7D). In addition, EdU staining was conducted and revealed that the number of cells in the DNA replication stage was significantly decreased in the OE + LY294002 group compared with the Ndrg2-overexpressed

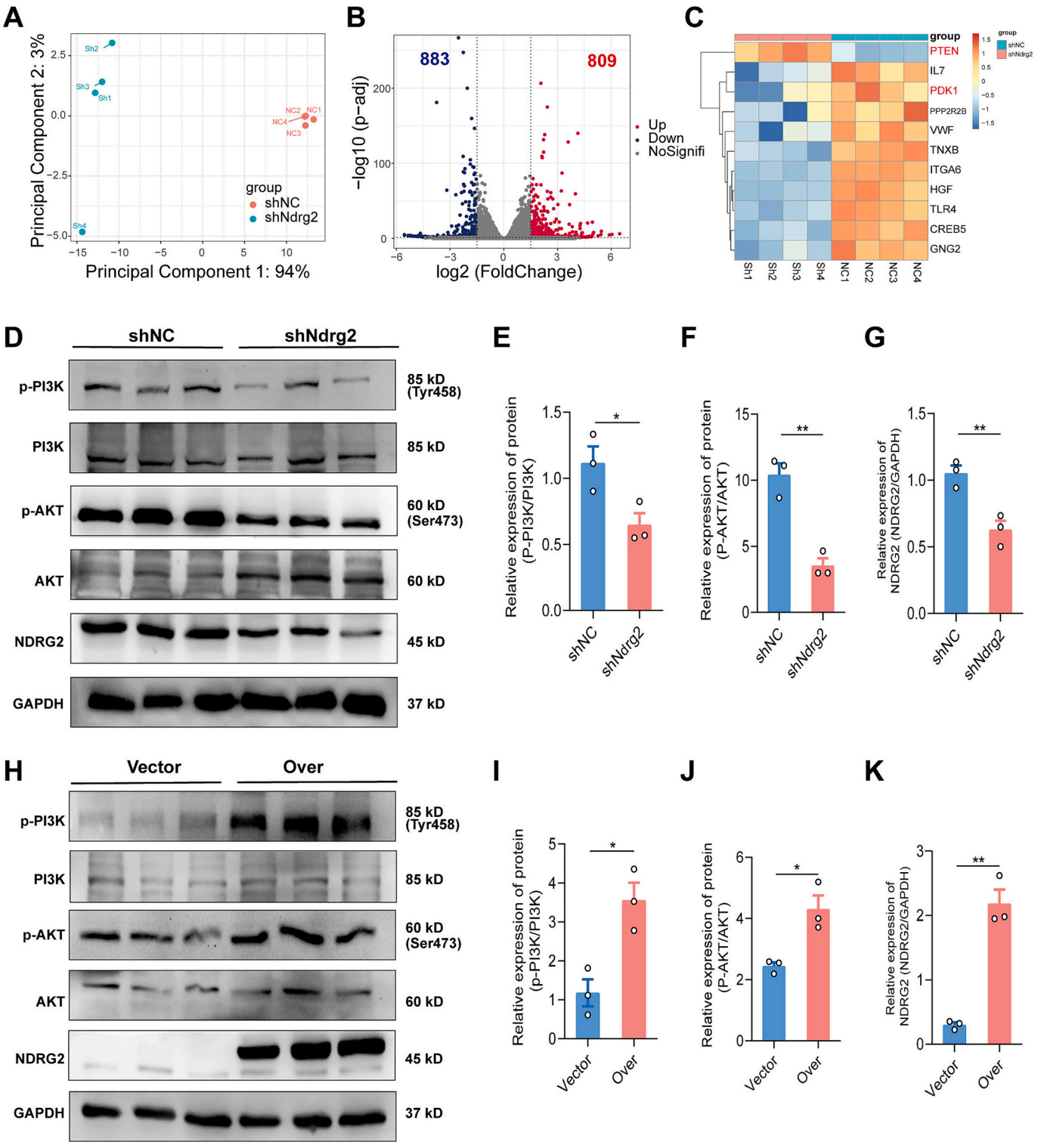

Fig. 6. PI3K/AKT pathway changed in Ndrg2-interfered fibroblasts. (A) PCA was performed to visualize the separation of shNdrg2 and shNC groups. (B) Volcano plot showing DEGs between shNdrg2 and shNC groups. (C) Heatmap showing expression profile of genes related to PI3K/AKT signaling pathway. (D) Levels of phosphorylated and total PI3K and AKT were measured in fibroblasts treated with shNC or shNdrg2. (E-G) Data analysis of the western blot results using ImageJ; $n = 3$ per group. (H) Levels of phosphorylated and total PI3K and AKT were assessed in fibroblasts treated with Vector or Ndrg2-overexpressing adenovirus. (I-K) Semi-quantification of the western blot results using ImageJ; n = 3 per group. All data are presented as mean ± SEM. *$p < 0.05$; **$p < 0.01$. Data were analyzed using a two-tailed unpaired Student's *t*-test.

NFB group (Fig. 7E and F). The results of the Transwell assay indicated that in Ndrg2-overexpressed NFB, the number of invasive cells was dramatically decreased after the administration of LY294002 (Fig.7 G and H). Similarly, the wound-healing assay revealed that the capacity of migration was considerably reduced after the use of LY294002 in Ndrg2-overexpressed NFB (Fig. 7I and J). These results suggested Ndrg2 promotes the proliferation and migration of fibroblasts through the PI3K/AKT signaling pathway.

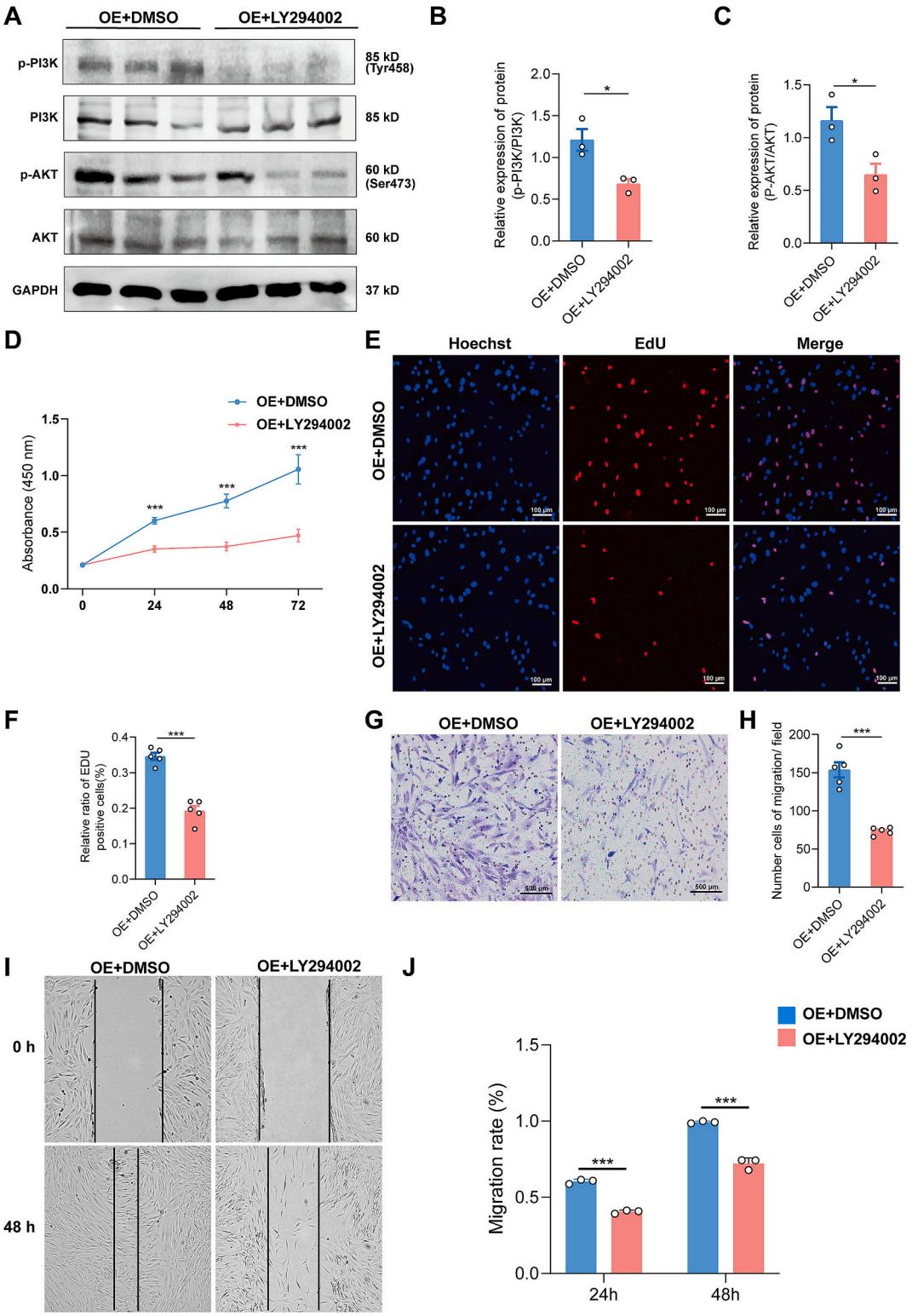

Fig. 7. LY294002 reversed the effects of overexpression of Ndrg2 on promoting the proliferation and migration of fibroblasts. (A) Representative western blotting images of phosphorylated and total PI3K and AKT in fibroblasts treated with Ndrg2-overexpressing (OE) adenovirus with Dimethyl sulfoxide (DMSO) or PI3K inhibitor (LY294002). (B-C) Data analysis of the western blot results using ImageJ; n = 3 per group. (D) The cell viability of fibroblasts treated with DMSO or LY294002 in Ndrg2 OE fibroblasts; n = 5 per group. (E) Representative images of EdU staining of fibroblasts treated with DMSO or LY294002 in Ndrg2 OE fibroblasts. Scale bar = 100 μm. (F) The relative ratio of EdU-positive cells in the OE + DMSO and OE + LY294002 groups; n = 5 fields per group. (G-H) Quantification analysis of cell migration per field (G) and representative images of Transwell invasion assay (H) in the OE + DMSO and OE + LY294002 groups; n = 5 fields per group. (I-J) Wound-healing assay was performed to detect the effect of cell migration in the OE + DMSO and OE + LY294002 groups. All data are presented as mean ± SEM. *$p < 0.05$; ***, $p < 0.001$. All data were analyzed using a two-tailed unpaired Student's *t*-test.

4. Discussion

In this study, we analyzed the effects of Ndrg2 on the proliferation and migration in vitro of fibroblasts and in vivo in a BLM-induced fibrosis mouse model. We revealed that Ndrg2 is a crucial regulatory component in skin fibrosis. Importantly, Ndrg2 overexpression could promote the proliferation and migration of fibroblasts through the PI3K/AKT signaling pathway, as presented in our summarized signaling diagram (Fig. 8). A PI3K inhibitor (LY294002) could reverse the effects of Ndrg2 overexpression in promoting the proliferation and migration of fibroblasts. This study provides a novel mechanism for the pathogenesis of HTS and presents a potential therapeutic target gene of Ndrg2 for HTS treatment.

As a member of the Ndrg family, Ndrg2 is a cellular stress response gene that not only plays a tumor suppressor role in various cancer types but also participates in cell proliferation, differentiation, apoptosis, and other processes [26–29]. In addition, Ndrg2 has been reported to be associated with fibrotic diseases. In a mouse model of liver fibrosis induced by dimethylnitrosamine, Ndrg2 overexpression could reduce the transcription and phosphorylation of Smad3, which blocked TGF-β1 signaling and inhibited the activation of hepatic stellate cells [30]. Furthermore, Ndrg2 could increase the ratio of matrix metallopeptidase 2 (MMP2) to tissue inhibitor of metalloproteinases (TIMPs), reduce the deposition of extracellular matrix, and alleviate liver fibrosis [31]. In another study, Ndrg2 could regulate the expression of TGF-β1 in LX-2 cells through the NF-κB pathway under hypoxia [32]. In the kidney, Ndrg2 modulated the fibrosis of renal tubular epithelial cells induced by TGF-β1 through the TGF-β1/Smad3 signaling pathway [33]. It has been reported that the human lens epithelial cells exhibits fibroblast-like morphological changes when Ndrg2 is overexpressed [23]. However, the role of Ndrg2 in skin fibrosis has not been reported.

In the present study, we found that Ndrg2 was upregulated in HTS compared with normal skin by western blot. It has been reported that Ndrg2 is a hypoxic stress response gene [34]. When human lung adenocarcinoma cells were subjected to hypoxia stimulation, the protein level of Ndrg2 gradually increased with the prolongation of hypoxia. The same phenomenon was also observed in HepGZ and skBR-3 cell lines [35]. In some way, the interior of HTS is hypoxic. On the one hand, when the extracellular matrix is excessively deposited, the microvasculature within the tissue is compressed, leading to a hypoxic microenvironment inside the scar [36]. On the other hand, excessive tissue proliferation leads to increased cellular metabolism and oxygen consumption, which also exacerbates hypoxia in the microenvironment [37]. Therefore, we hypothesized that the increased expression of Ndrg2 in HTS may be related to the hypoxic stress and hypoxic microenvironment in the tissue.

Animal models are important tools for studying scar treatment and pathogenesis. Because of the phylogenetic differences among various species, there are certain limitations in the selection of nude mice, rabbits, mice, or pigs for modeling. After referring to the literature [38–40], we used bleomycin to induce skin fibrosis in a mouse model and chose Ndrg2 knockout mice as the experimental subjects to investigate the effect of Ndrg2 deletion on scar formation. Bleomycin can activate the expression of TGF- β and other pro-fibrotic factors [41,42], and the fibrotic skin of mice has similar pathological characteristics to human HTS, such as inflammatory cell infiltration, collagen deposition and skin appendage atrophy [43]. The method of subcutaneous injection was relatively simple and economical. The results indicated that the protein expression of Ndrg2 in the fibrotic skin of mice was significantly increased compared with that in normal skin, which again proved that Ndrg2 was related to skin fibrosis. In addition, Ndrg2 knockout mice exhibited significant resistance to BLM-induced skin fibrosis. After injection of bleomycin, the collagen I in the skin of KO mice was notably lower than that of control mice, indicating that Ndrg2 can affect the synthesis of collagen I in the skin. Ndrg2 deficiency can alleviate skin fibrosis caused by BLM in mice, which provided strong evidence of the pro-fibrosis effect of Ndrg2 in scar formation. Many studies have utilized $Col1a2^{CreER}$ or $S100a4^{CreRT}$ mice to generate fibroblast-specific gene knockout mice to study the roles of specific genes in fibroblast [44]. Experiments at later timepoints are needed to establish fibroblast-specific Ndrg2 knockout mice to study the advanced mechanism.

Subsequently, we further investigated the effect of Ndrg2 on the biological behavior of fibroblasts. The migration of fibroblasts is assumed to play a crucial role in the local progression of fibrosis. The results of wound-healing and Transwell assay indicated that Ndrg2 knockdown significantly inhibited the migration of HFB, whereas Ndrg2 overexpression promoted the migration of NFB. The CCK-8 and EdU assay revealed that Ndrg2 knockdown significantly inhibited the proliferation of HFB, whereas NFB exhibited the opposite trends when Ndrg2 was overexpressed. These results provide strong evidence that

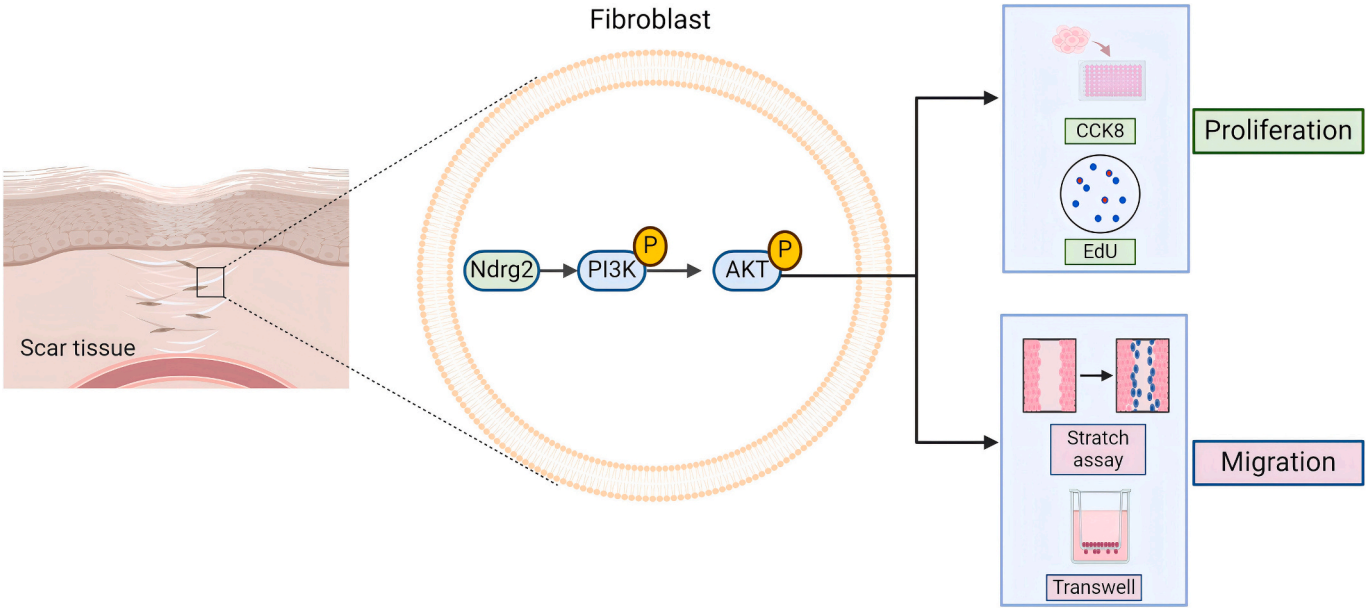

Fig. 8. Schematic diagram summarizing the role of Ndrg2 in promoting skin fibrosis in HFB.
Ndrg2 plays a crucial role in HFB. Ndrg2 promotes the proliferation and migration of fibroblasts through the PI3K/AKT signaling pathway.

Ndrg2 promotes fibrosis through fibroblasts.

The PI3K/AKT signaling pathway is one of the most classical intracellular signal transduction pathways, which is of great significance for the regulation of cell proliferation [45,46], migration [47,48], transformation [49], metabolism [50], and apoptosis [51]. Studies have shown that the Ndrg2 gene is closely related to PI3K/AKT pathway and plays a regulatory role in various diseases. For example, in the process of myocardial ischemia-reperfusion, Ndrg2 can act as a substrate and phosphorylated protein of Akt to mediate the protective effect of insulin on myocardium [52]. Ndrg2 can also affect the apoptosis and autophagy of mouse neurons by regulating the PI3K/AKT pathway, which provides a target for the treatment of ischemic stroke [53]. In addition, the PI3K/AKT signaling pathway is closely associated with HTS as we previous reported [25]. In the present study, Ndrg2 interference inhibited signal transduction of the PI3K/AKT pathway in HFB. Consistent with our results, the PI3K/AKT signaling pathway was activated after overexpressing Ndrg2. In addition, we found that the proliferation and migration of Ndrg2-overexpressed NFB was significantly attenuated after the administration of PI3K signaling inhibitor (LY294002). These results suggest that Ndrg2 regulated the PI3K/AKT signaling pathway to promote the proliferation and migration of fibroblasts in skin fibrosis.

However, some limitations must be acknowledged in this study. First, this study is limited in size, although we utilized the clinical, animal and cell experiments to enhance our results. Second, wortmannin and other novel PI3K pathway inhibitors should be employed in the further study, although LY294002 and wortmannin are the earliest and still widely employed inhibitors of PI3K in many studies. Finally, we noticed further studies are needed to investigate the direct effect between Ndrg2 and PI3K/AKT signaling pathway on hypertrophic scar and discover potential intervention targets.

5. Conclusions

In conclusion, our study reveals the function and mechanism of Ndrg2 in skin fibrosis. We reported the upregulation of Ndrg2 in HTS of human and BLM-induced fibrosis mouse model and demonstrated the pro-fibrotic effects of Ndrg2 using in vivo experiments. The results also presented evidence that Ndrg2 was involved in the process of fibrosis by regulating the PI3K/AKT pathway. This study provides a novel therapeutic target of Ndrg2 for HTS and elucidates the particular mechanism underlying the clinical treatment of HTS.

Ethics approval and consent to participate

The human experiments performed in this study were approved by the Medical and Ethics Committees of the Fourth Medical Center of Chinese PLA General Hospital (2023KY140-KS001) and the animal experiments were approved by the Experimental Animal of Committee Fourth Medical Center, Chinese PLA General Hospital (SQ2023662).

Consent to publish

Not applicable.

Funding

This study was supported by Incubation Fundation of Shandong Provincial Hospital (2024FY075).

CRediT authorship contribution statement

Boya Yu: Writing – original draft, Methodology. **Yalei Cao:** Validation, Conceptualization. **Pianpian Lin:** Methodology, Conceptualization. **Lixia Zhang:** Supervision. **Minliang Chen:** Writing – review & editing, Data curation, Conceptualization.

Declaration of competing interest

The authors declare no competing interests.

Acknowledgements

None.

Appendix A. Supplementary data

Supplementary data to this article can be found online at https://doi.org/10.1016/j.cellsig.2025.111659.

Data availability

All data generated or analyzed in this study are included in this article and its supplementary materials.

References

[1] B. Kuehlmann, C.A. Bonham, I. Zucal, L. Prantl, G.C. Gurtner, Mechanotransduction in wound healing and fibrosis, J. Clin. Med. 9 (5) (2020).
[2] J. Zhang, Y. Li, X. Bai, Y. Li, J. Shi, D. Hu, Recent advances in hypertrophic scar, Histol. Histopathol. 33 (1) (2018) 27–39.
[3] Z.C. Wang, W.Y. Zhao, Y. Cao, Y.Q. Liu, Q. Sun, P. Shi, J.Q. Cai, X.Z. Shen, W. Q. Tan, The roles of inflammation in keloid and hypertrophic scars, Front. Immunol. 11 (2020) 603187.
[4] R. Ogawa, T. Dohi, M. Tosa, M. Aoki, S. Akaishi, The latest strategy for keloid and hypertrophic scar prevention and treatment: the Nippon medical school (NMS) Protocol, J. Nippon Med. Sch. 88 (1) (2021) 2–9.
[5] R. Ogawa, The Most current algorithms for the treatment and prevention of hypertrophic scars and keloids: a 2020 update of the algorithms published 10 years ago, Plast. Reconstr. Surg. 149 (1) (2022) 79e–94e.
[6] H.J. Lee, Y.J. Jang, Recent understandings of biology, prophylaxis and treatment strategies for hypertrophic scars and keloids, Int. J. Mol. Sci. 19 (3) (2018).
[7] S. Knoedler, S. Broichhausen, R. Guo, R. Dai, L. Knoedler, M. Kauke-Navarro, F. Diatta, B. Pomahac, H.G. Machens, D. Jiang, et al., Fibroblasts - the cellular choreographers of wound healing, Front. Immunol. 14 (2023) 1233800.
[8] M.F. Griffin, H.E. desJardins-Park, S. Mascharak, M.R. Borrelli, M.T. Longaker, Understanding the impact of fibroblast heterogeneity on skin fibrosis, Dis. Model. Mech. 13 (6) (2020).
[9] Y. Li, Z. Yu, D. Zhao, D. Han, Corilagin alleviates hypertrophic scars via inhibiting the transforming growth factor (TGF)-β/Smad signal pathway, Life Sci. 277 (2021) 119483.
[10] F. Ma, J. Shen, H. Zhang, Z. Zhang, A. Yang, J. Xiong, Y. Jiao, Z. Bai, S. Ma, H. Zhang, et al., A novel lncRNA FPASL regulates fibroblast proliferation via the PI3K/AKT and MAPK signaling pathways in hypertrophic scar, Acta Biochim. Biophys. Sin. Shanghai 55 (2) (2022) 274–284.
[11] X. Bai, T. He, J. Liu, Y. Wang, L. Fan, K. Tao, J. Shi, C. Tang, L. Su, D. Hu, Loureirin B inhibits fibroblast proliferation and extracellular matrix deposition in hypertrophic scar via TGF-β/Smad pathway, Exp. Dermatol. 24 (5) (2015) 355–360.
[12] X. Zhou, S. Lin, HOXC10 promotes hypertrophic scar fibroblast fibrosis through the regulation of STMN2 and the TGF-β/Smad signaling pathway, Histochem. Cell Biol. 162 (5) (2024) 403–413.
[13] T. He, Y. Zhang, Y. Liu, H. Wang, W. Zhang, J. Liu, N. Li, Y. Li, L. Wang, S. Xie, et al., MicroRNA-494 targets PTEN and suppresses PI3K/AKT pathway to alleviate hypertrophic scar formation, J. Mol. Histol. 50 (4) (2019) 315–323.
[14] Y. Zhi, H. Wang, B. Huang, G. Yan, L.Z. Yan, W. Zhang, J. Zhang, Panax Notoginseng Saponins suppresses TRPM7 via the PI3K/AKT pathway to inhibit hypertrophic scar formation in vitro, Burns 47 (4) (2021) 894–905.
[15] X. Liu, T. Niu, X. Liu, W. Hou, J. Zhang, L. Yao, Microarray profiling of HepG2 cells ectopically expressing NDRG2, Gene 503 (1) (2012) 48–55.
[16] V. Melotte, X. Qu, M. Ongenaert, W. van Criekinge, A.P. de Bruïne, H.S. Baldwin, M. van Engeland, The N-myc downstream regulated gene (NDRG) family: diverse functions, multiple applications, FASEB J. 24 (11) (2010) 4153–4166.
[17] S. Wang, N. Chen, N. Dong, L. Lu, L. Liu, L. Zhang, Adenovirus siMDM2 and NDRG2 gene therapy inhibits cell proliferation and induces apoptosis of squamous cell carcinoma, Cell Biochem. Biophys. 73 (2) (2015) 513–518.
[18] X. Xu, J. Li, X. Sun, Y. Guo, D. Chu, L. Wei, X. Li, G. Yang, X. Liu, L. Yao, et al., Tumor suppressor NDRG2 inhibits glycolysis and glutaminolysis in colorectal cancer cells by repressing c-Myc expression, Oncotarget 6 (28) (2015) 26161–26176.
[19] V.C. Foletta, M.J. Prior, N. Stupka, K. Carey, D.H. Segal, S. Jones, C. Swinton, S. Martin, D. Cameron-Smith, K.R. Walder, NDRG2, a novel regulator of myoblast proliferation, is regulated by anabolic and catabolic factors, J. Physiol. 587 (Pt 7) (2009) 1619–1634.
[20] T. Ichikawa, S. Nakahata, M. Fujii, H. Iha, K. Morishita, Loss of NDRG2 enhanced activation of the NF-κB pathway by PTEN and NIK phosphorylation for ATL and other cancer development, Sci. Rep. 5 (2015) 12841.

[21] D.G. Lee, S.H. Lee, J.S. Kim, J. Park, Y.L. Cho, K.S. Kim, D.Y. Jo, I.C. Song, N. Kim, H.J. Yun, et al., Loss of NDRG2 promotes epithelial-mesenchymal transition of gallbladder carcinoma cells through MMP-19-mediated slug expression, J. Hepatol. 63 (6) (2015) 1429–1439.
[22] J. Yang, J. Zheng, L. Wu, M. Shi, H. Zhang, X. Wang, N. Xia, D. Wang, X. Liu, L. Yao, et al., NDRG2 ameliorates hepatic fibrosis by inhibiting the TGF-β1/Smad pathway and altering the MMP2/TIMP2 ratio in rats, PLoS One 6 (11) (2011) e27710.
[23] Z.F. Zhang, J. Zhang, Y.N. Hui, M.H. Zheng, X.P. Liu, P.F. Kador, Y.S. Wang, L. B. Yao, J. Zhou, Up-regulation of NDRG2 in senescent lens epithelial cells contributes to age-related cataract in human, PLoS One 6 (10) (2011) e26102.
[24] J. Wang, M. Zhao, H. Zhang, F. Yang, L. Luo, K. Shen, X. Wang, Y. Li, J. Zhang, J. Zhang, et al., KLF4 alleviates hypertrophic scar fibrosis by directly activating BMP4 transcription, Int. J. Biol. Sci. 18 (8) (2022) 3324–3336.
[25] B. Yu, Y. Cao, S. Li, R. Bai, G. Zhou, Q. Fu, L. Liang, W. Gu, L. Zhang, M. Chen, Identification and validation of CRLF1 and NRG1 as immune-related signatures in hypertrophic scar, Genomics 116 (2) (2024) 110797.
[26] K. Kang, S. Nam, B. Kim, J.H. Lim, Y. Yang, M.S. Lee, J.S. Lim, Inhibition of osteoclast differentiation by overexpression of NDRG2 in monocytes, Biochem. Biophys. Res. Commun. 468 (4) (2015) 611–616.
[27] N.R. Nichols, Ndrg2, a novel gene regulated by adrenal steroids and antidepressants, is highly expressed in astrocytes, Ann. N. Y. Acad. Sci. 1007 (2003) 349–356.
[28] J. Hu, L. Feng, M. Ren, Y. Zhao, G. Lu, X. Lu, Y. Li, X. Wang, X. Bu, S. Wang, et al., Colorectal Cancer cell differentiation is dependent on the repression of aerobic glycolysis by NDRG2-TXNIP Axis, Dig. Dis. Sci. 67 (8) (2022) 3763–3772.
[29] X.L. Hu, X.P. Liu, Y.C. Deng, S.X. Lin, L. Wu, J. Zhang, L.F. Wang, X.B. Wang, X. Li, L. Shen, et al., Expression analysis of the NDRG2 gene in mouse embryonic and adult tissues, Cell Tissue Res. 325 (1) (2006) 67–76.
[30] H. Huang, K. Wang, Q. Liu, F. Ji, H. Zhou, S. Fang, J. Zhu, The active constituent from Gynostemma Pentaphyllum prevents liver fibrosis through regulation of the TGF-β1/NDRG2/MAPK Axis, Front. Genet. 11 (2020) 594824.
[31] D.C. Lee, Y.K. Kang, W.H. Kim, Y.J. Jang, D.J. Kim, I.Y. Park, B.H. Sohn, H.A. Sohn, H.G. Lee, J.S. Lim, et al., Functional and clinical evidence for NDRG2 as a candidate suppressor of liver cancer metastasis, Cancer Res. 68 (11) (2008) 4210–4220.
[32] H.Z. Ba, Z.H. Liang, H.S. Kim, W. Cao, TGF-β1 can be regulated by NDRG2 via the NF-κB pathway in hypoxia-induced liver fibrosis, Ann. Transl. Med. 9 (6) (2021) 505.
[33] Z. Jin, C. Gu, F. Tian, Z. Jia, J. Yang, NDRG2 knockdown promotes fibrosis in renal tubular epithelial cells through TGF-β1/Smad3 pathway, Cell Tissue Res. 369 (3) (2017) 603–610.
[34] L. Wang, N. Liu, L. Yao, F. Li, J. Zhang, Y. Deng, J. Liu, S. Ji, A. Yang, H. Han, et al., NDRG2 is a new HIF-1 target gene necessary for hypoxia-induced apoptosis in A549 cells, Cell. Physiol. Biochem. 21 (1–3) (2008) 239–250.
[35] G.Q. Wu, X.P. Liu, L.F. Wang, W.H. Zhang, J. Zhang, K.Z. Li, K.F. Dou, X.F. Zhang, L.B. Yao, Induction of apoptosis of HepG2 cells by NDRG2, Xi Bao Yu Fen Zi Mian Yi Xue Za Zhi 19 (4) (2003) 357–360.
[36] B.O. Mofikoya, W.L. Adeyemo, A.O. Ugburo, An overview of biological basis of pathologic scarring, Niger. Postgrad. Med. J. 19 (1) (2012) 40–45.
[37] R.K. Thapa, D.J. Margolis, K.L. Kiick, M.O. Sullivan, Enhanced wound healing via collagen-turnover-driven transfer of PDGF-BB gene in a murine wound model, ACS Appl. Bio Mater. 3 (6) (2020) 3500–3517.
[38] M.L. Ramos, A. Gragnani, L.M. Ferreira, Is there an ideal animal model to study hypertrophic scarring? J. Burn Care Res. 29 (2) (2008) 363–368.
[39] J. Li, Y. Li, Y. Wang, X. He, J. Wang, W. Cai, Y. Jia, D. Xiao, J. Zhang, M. Zhao, et al., Overexpression of miR-101 suppresses collagen synthesis by targeting EZH2 in hypertrophic scar fibroblasts, Burns Trauma 9 (2021) tkab038.
[40] Y.I. Lee, J.E. Shim, J. Kim, W.J. Lee, J.W. Kim, K.H. Nam, J.H. Lee, WNT5A drives interleukin-6-dependent epithelial-mesenchymal transition via the JAK/STAT pathway in keloid pathogenesis, Burns Trauma 10 (2022) tkac023.
[41] Y. Zhang, L. Shen, H. Zhu, K. Dreissigacker, D. Distler, X. Zhou, A.H. Györfi, C. Bergmann, X. Meng, C. Dees, et al., PGC-1α regulates autophagy to promote fibroblast activation and tissue fibrosis, Ann. Rheum. Dis. 79 (9) (2020) 1227–1233.
[42] O. Khazri, K. Charradi, F. Limam, M.V. El May, E. Aouani, Grape seed and skin extract protects against bleomycin-induced oxidative stress in rat lung, Biomed. Pharmacother. 81 (2016) 242–249.
[43] T. Yamamoto, S. Takagawa, I. Katayama, K. Yamazaki, Y. Hamazaki, H. Shinkai, K. Nishioka, Animal model of sclerotic skin. I: local injections of bleomycin induce sclerotic skin mimicking scleroderma, J. Invest. Dermatol. 112 (4) (1999) 456–462.
[44] I. Tuleta, A. Hanna, C. Humeres, J.T. Aguilan, S. Sidoli, F. Zhu, N.G. Frangogiannis, Fibroblast-specific TGF-β signaling mediates cardiac dysfunction, fibrosis, and hypertrophy in obese diabetic mice, Cardiovasc. Res. 120 (16) (2024) 2047–2063.
[45] L. Ma, R. Zhang, D. Li, T. Qiao, X. Guo, Fluoride regulates chondrocyte proliferation and autophagy via PI3K/AKT/mTOR signaling pathway, Chem. Biol. Interact. 349 (2021) 109659.
[46] H. Zhao, C. Li, L. Li, J. Liu, Y. Gao, K. Mu, D. Chen, A. Lu, Y. Ren, Z. Li, Baicalin alleviates bleomycin-induced pulmonary fibrosis and fibroblast proliferation in rats via the PI3K/AKT signaling pathway, Mol. Med. Rep. 21 (6) (2020) 2321–2334.
[47] J. Qu, J. Li, Y. Zhang, R. He, X. Liu, K. Gong, L. Duan, W. Luo, Z. Hu, G. Wang, et al., AKR1B10 promotes breast cancer cell proliferation and migration via the PI3K/AKT/NF-κB signaling pathway, Cell Biosci. 11 (1) (2021) 163.
[48] Z. You, Z. Yang, S. Cao, S. Deng, Y. Chen, The novel KLF4/BIG1 regulates LPS-mediated neuro-inflammation and migration in BV2 cells via PI3K/Akt/NF-kB signaling pathway, Neuroscience 488 (2022) 102–111.
[49] T. Li, T. Liu, X. Chen, L. Li, M. Feng, Y. Zhang, L. Wan, C. Zhang, W. Yao, Microglia induce the transformation of A1/A2 reactive astrocytes via the CXCR7/PI3K/Akt pathway in chronic post-surgical pain, J. Neuroinflammation 17 (1) (2020) 211.
[50] G. Hoxhaj, B.D. Manning, The PI3K-AKT network at the interface of oncogenic signalling and cancer metabolism, Nat. Rev. Cancer 20 (2) (2020) 74–88.
[51] T. Ersahin, N. Tuncbag, R. Cetin-Atalay, The PI3K/AKT/mTOR interactive pathway, Mol. BioSyst. 11 (7) (2015) 1946–1954.
[52] Z. Sun, G. Tong, N. Ma, J. Li, X. Li, S. Li, J. Zhou, L. Xiong, F. Cao, L. Yao, et al., NDRG2: a newly identified mediator of insulin cardioprotection against myocardial ischemia-reperfusion injury, Basic Res. Cardiol. 108 (3) (2013) 341.
[53] Y. Wang, B. Wang, Y. Liu, Y. Guo, H. Lu, X. Liu, Inhibition of PI3K/Akt/mTOR signaling by NDRG2 contributes to neuronal apoptosis and autophagy in ischemic stroke, J. Stroke Cerebrovasc. Dis. 32 (3) (2023) 106984.